

Evidence of Strong Electron Correlations in γ -Iron

Yoshiro KAKEHASHI*, M. Atiqur R. PATOARY, and Toshihito TAMASHIRO

*Department of Physics and Earth Sciences, Faculty of Science, University of the Ryukyus,
1 Senbaru, Nishihara, Okinawa, 903-0213, Japan*

Single-particle excitation spectra of γ -Fe in the paramagnetic state have been investigated by means of the first-principles dynamical coherent potential approximation theory which has recently been developed. It is found that the central peak in the density of states consisting of the t_{2g} bands is destroyed by electron correlations, and the Mott-Hubbard type correlated bands appear. The results indicate that the γ -Fe can behave as correlated electrons at high temperatures.

KEYWORDS: single-particle excitation spectra, electron correlations, Mott-Hubbard band, γ -Fe, γ -Mn, Fe-pnictides, XPS, BIS

The 3d transition metals are wellknown to behave as a typical itinerant electron system in which the ground-state properties are explained well by the band theory.¹ The cohesive properties such as lattice parameters and bulk moduli, and the ground-state magnetizations are in fact quantitatively explained by the density functional theory for band calculations. On the other hand, excitations in these metals are often not explained by the band theory. The magnetic properties of Fe, Co, and Ni, for examples, show at finite temperatures the local moment behaviors as explained by the Heisenberg model.² Excitation spectra of Ni observed by means of the X-ray photoelectron spectroscopy (XPS) are wellknown to show a d -band narrowing and a satellite peak at 6 eV below the Fermi level,³ which can not be obtained by an independent-particle picture. These results indicate that the effects of electron correlations in transition metals strongly depends on the details of parameters controlling the physical quantities. Small change in the key parameters might cause anomalous behaviors such as high-temperature superconductivity which has recently been found in the iron-arsenide system.⁴ In order to clarify the characteristic features of transition metal systems, one has to examine their electronic properties on the basis of realistic band theory which takes into account electron correlations.

In this letter, we present our numerical results of single-particle excitation spectra for γ -Fe in the paramagnetic state, which are obtained by the first-principles dynamical coherent potential approximation (CPA) theory, and demonstrate that γ -Fe can be regarded as a strongly correlated electron system at high temperatures, though their ground-state properties are believed to be well explained by a band theory.⁵⁻⁷

*E-mail address: yok@sci.u-ryukyu.ac.jp, to be published in J. Phys. Soc. Jpn. **78** No. 9 (2009).

The first-principles dynamical CPA theory⁸ is the dynamical CPA⁹ combined with the first principle tight-binding (TB) linear muffin-tin orbital (LMTO) Hamiltonian.¹⁰ The former is a dynamical version of the single-site spin fluctuation theory developed by Cyrot,¹¹ Hubbard,¹² and Hasegawa¹³ since early in the 1970, and has recently been shown¹⁴ to be equivalent to the dynamical mean field theory (DMFT).¹⁵ The theory describes the electronic and magnetic properties at finite temperatures efficiently taking into account the dynamical corrections to the spin and charge fluctuations. Note that unlike the early quantum Monte-Carlo (QMC) calculations combined with the DMFT¹⁶ the present approach can treat the transverse spin fluctuations for arbitrary d electron number.

We adopt the TB-LMTO Hamiltonian H_0 plus the following intraatomic Coulomb interactions H_1 between d electrons.

$$H_1 = \sum_i \left[\sum_m U_0 \hat{n}_{ilm\uparrow} \hat{n}_{ilm\downarrow} + \sum_{m>m'} (U_1 - \frac{1}{2}J) \hat{n}_{ilm} \hat{n}_{ilm'} - \sum_{m>m'} J \hat{s}_{ilm} \cdot \hat{s}_{ilm'} \right]. \quad (1)$$

Here U_0 (U_1) and J are the intra-orbital (inter-orbital) Coulomb interaction and the exchange interaction, respectively. $\hat{n}_{ilm\sigma}$ is the number operator for electrons with orbital lm and spin σ on site i . \hat{n}_{ilm} (\hat{s}_{ilm}) with $l = 2$ is the charge (spin) density operator for d electrons on site i and orbital m .

In the dynamical CPA,⁸ we transform the interacting Hamiltonian H_1 into a dynamical potential v in the free energy adopting the functional integral method, and expand the free energy with respect to sites after having introduced a uniform medium, (*i.e.* a coherent potential) $\Sigma_{L\sigma}(i\omega_n)$. Note that $L = (l, m)$, and ω_n denotes the Matsubara frequency. The first term in the expansion is the free energy for a uniform medium, $\tilde{\mathcal{F}}[\Sigma]$. The second term is an impurity contribution to the free energy. The dynamical CPA neglects the higher-order terms, so that the free energy per atom is given by

$$\mathcal{F}_{\text{CPA}} = \tilde{\mathcal{F}}[\Sigma] - \beta^{-1} \ln C \int d\xi e^{-\beta E_{\text{eff}}(\xi)}. \quad (2)$$

Here β is the inverse temperature. C is a normalization constant. ξ denotes the static field variable on a site. $E_{\text{eff}}(\xi)$ is an effective potential projected onto the static field ξ . It consists of the static term $E_{\text{st}}(\xi)$ and the dynamical correction term $E_{\text{dyn}}(\xi)$. The latter is given by a Gaussian average of the determinant D of the scattering matrix due to dynamical potential as follows.

$$e^{-\beta E_{\text{dyn}}(\xi)} = \overline{D} = \overline{\det[1 - (v - v_0)\tilde{g}]}. \quad (3)$$

Here $(v)_{Ln\sigma L'n'\sigma'} = v_{L\sigma\sigma'}(i\omega_n - i\omega_{n'})\delta_{LL'}$ ($(v_0)_{Ln\sigma L'n'\sigma'} = v_{L\sigma\sigma'}(0)\delta_{LL'}\delta_{nn'}$) is the dynamical (static) potential, and $(\tilde{g})_{Ln\sigma L'n'\sigma'}$ is the Green function in the static approximation. The overline denotes the Gaussian average with respect to the field variables.

In order to treat the dynamical potential analytically, we expand the dynamical part of the effective potential with respect to the frequency ν of $v_{L\sigma\sigma'}(i\omega_\nu)$, and neglect the mode-

mode coupling terms. This is called the harmonic approximation, and $\bar{D} \approx 1 + \sum_{\nu} (\bar{D}_{\nu} - 1)$. Here D_{ν} is a sub-matrix of D in which the dynamical potential v has been replaced by its ν component only.

The effective medium (*i.e.*, the coherent potential) can be determined by the stationary condition $\delta\mathcal{F}_{\text{CPA}}/\delta\Sigma = 0$. This yields the CPA equation as

$$\langle G_{L\sigma}(\boldsymbol{\xi}, i\omega_n) \rangle = F_{L\sigma}(i\omega_n) . \quad (4)$$

Note that $\langle \rangle$ at the l.h.s. is a classical average taken with respect to the effective potential $E_{\text{eff}}(\boldsymbol{\xi})$, $F_{L\sigma}(i\omega_n) = [(i\omega_n - \mathbf{H}_0 - \boldsymbol{\Sigma})^{-1}]_{iL\sigma iL\sigma}$ is the coherent Green function, where $(\mathbf{H}_0)_{iL\sigma jL'\sigma}$ is the one-electron TB-LMTO Hamiltonian matrix, and $(\boldsymbol{\Sigma})_{iL\sigma jL'\sigma} = \Sigma_{L\sigma}(i\omega_n)\delta_{ij}\delta_{LL'}$. Furthermore, $G_{L\sigma}(\boldsymbol{\xi}, i\omega_n)$ is the impurity Green function given by

$$G_{L\sigma}(\boldsymbol{\xi}, i\omega_n) = \tilde{g}_{L\sigma L\sigma}(i\omega_n) + \frac{\sum_{\nu} \frac{\delta\bar{D}_{\nu}(\boldsymbol{\xi})}{\kappa_{L\sigma}(i\omega_n)\delta\Sigma_{L\sigma}(i\omega_n)}}{1 + \sum_{\nu} (\bar{D}_{\nu}(\boldsymbol{\xi}) - 1)} . \quad (5)$$

Here the first term at the r.h.s. is the Green function in the static approximation. The second term is the dynamical corrections, and $\kappa_{L\sigma}(i\omega_n) = 1 - F_{L\sigma}(i\omega_n)^{-2}\delta F_{L\sigma}(i\omega_n)/\delta\Sigma_{L\sigma}(i\omega_n)$.

Solving the CPA equation (4) self-consistently, we obtain the effective medium $\Sigma_{L\sigma}(i\omega_n)$. The density of states (DOS) for the single-particle excitation spectrum is obtained by means of a numerical analytic continuation of the coherent potential. In the numerical calculations, we expanded the dynamical correction term $\bar{D}_{\nu}(\boldsymbol{\xi})$ in Eqs. (3) and (5) with respect to the

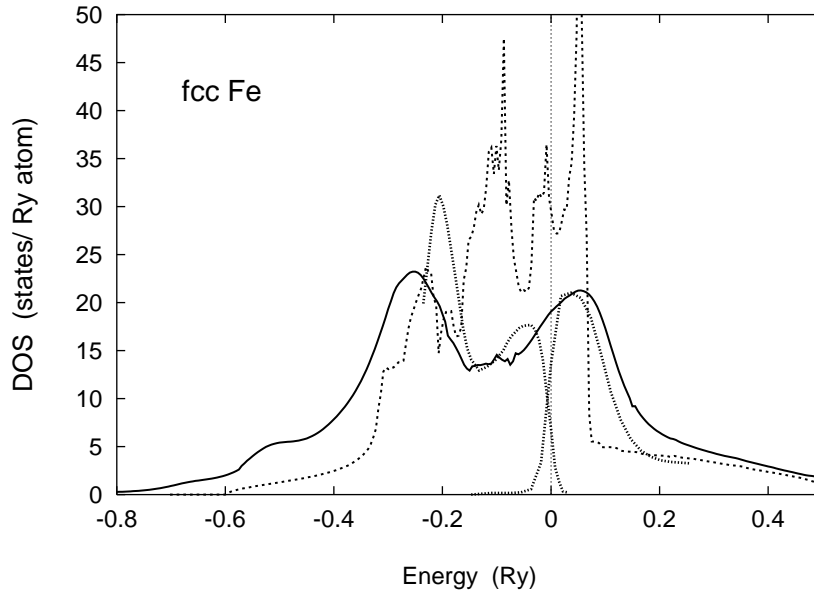


Fig. 1. Density of states (DOS) as the single-particle excitations for γ -Fe in the paramagnetic state calculated by the dynamical CPA (solid curve). The DOS in the LDA is shown by dashed curve. The BIS¹⁷ and XPS¹⁸ data are shown by dotted curves.

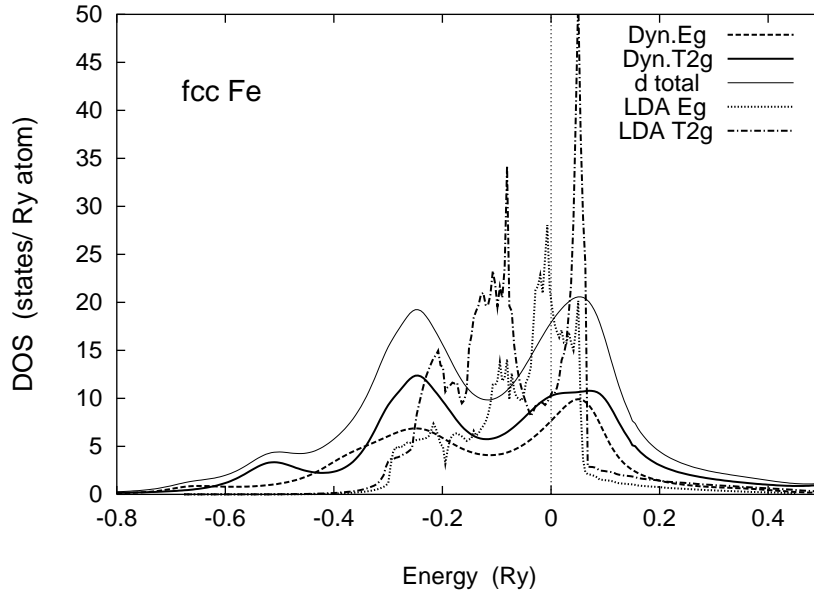


Fig. 2. Partial d DOS for e_g (dashed curve) and t_{2g} (solid curve) electrons. The total d DOS are shown by thin solid curves. The partial DOS in the LDA are shown by dotted curve (e_g) and dot-dashed curve (t_{2g}).

Coulomb interactions as $\overline{D}_\nu(\boldsymbol{\xi}) = 1 + \overline{D}_\nu^{(1)}(\boldsymbol{\xi}) + \overline{D}_\nu^{(2)}(\boldsymbol{\xi}) + \overline{D}_\nu^{(3)}(\boldsymbol{\xi}) + \overline{D}_\nu^{(4)}(\boldsymbol{\xi}) + \dots$, and calculated the r.h.s. up to the second order exactly as has been made in our previous calculations.⁸ In addition to the second-order terms, the third and fourth order terms are taken into account approximately in the present calculations by using an asymptotic approximation.⁹ We have obtained the TB-LMTO Hamiltonian at the observed lattice constant 6.928 a.u. at 1440 K using the local density approximation (LDA) in the density functional theory. The average Coulomb and exchange energy parameters (\overline{U} and J) for Fe are taken from the LDA+ U band calculations¹⁹; $(\overline{U}, J) = (0.169, 0.066)$. U_0 and U_1 are obtained from the relations $U_0 = \overline{U} + 8J/5$ and $U_1 = \overline{U} - 2J/5$.

We calculated the DOS for γ -Fe in the paramagnetic state at high temperatures ($T = 2000\text{K}$) where the present theory works best. The results are presented in Fig. 1. The fcc DOS in the LDA is characterized by the main peak near the top of d bands, the central peak around $\omega = -0.1$ Ry, and the third peak near the Fermi level. The first two peaks originate in the t_{2g} bands and the third one is due to the e_g bands. In the dynamical CPA calculations, the central peak is destroyed by electron correlations and the DOS shows the two peaks. The two peak structure is more explicitly found in the partial d DOS for e_g and t_{2g} orbitals as shown in Fig. 2. Both local DOS show a dip at $\omega = -0.1$ Ry. Especially the central peak of the t_{2g} bands in the LDA disappears due to electron correlations and the spectral weight moves to the lower and higher energy regions (*i.e.*, $\omega \lesssim -0.3$ Ry and $\omega \gtrsim 0.1$ Ry). These changes in the DOS are caused by a strong scattering peak of $-\text{Im}\Sigma_{L\sigma}(\omega + i\delta)$ around $\omega = -0.1$ Ry where

the central peak of the t_{2g} band in the LDA is located, and also by a change of the energy shift $\text{Re}\Sigma_{L\sigma}(\omega + i\delta)$ in sign; $\text{Re}\Sigma_{L\sigma}(\omega + i\delta) < 0$ for $\omega < -0.1$ Ry and $\text{Re}\Sigma_{L\sigma}(\omega + i\delta) > 0$ for $\omega > -0.1$ Ry. The two peaks at $\omega = -0.25$ and $\omega = 0.05$ Ry in the DOS are therefore considered to be the lower and upper Mott-Hubbard bands as found in the half-filled Hubbard model.

There is no experimental data for the bulk γ -Fe at high temperatures as far as we know. The BIS experimental data for 8 fcc Fe monolayers on Cu (100) surface at room temperature¹⁷ are consistent with our results as shown in Fig. 1. The photoemission data¹⁸ for 5 fcc Fe monolayers on Cu (100) are also shown in the figure. The peak at $\omega = -0.205$ Ry is usually interpreted to be due to the emission from the bulk Cu substrate. Another interpretation is that both the lower Hubbard bands for Fe and the Cu-substrate bands are superposed. Assuming the latter, the present results are consistent with the experimental data.

We have also performed the DOS calculations for γ -Mn to make sure the formation of the Mott-Hubbard bands in the fcc transition metals. We adopted the average Coulomb and exchange parameters $(\bar{U}, J) = (0.192, 0.061)$, which are taken from the LDA + U calculations with use of the Hartree-Fock-Slater potentials²⁰ and from the atomic calculations,²¹ respectively. We find again the two-peak structure in the DOS as shown in Fig. 3 when the dynamical CPA is applied. The energy difference between the lower peak and the upper one is larger than that of γ -Fe by about 0.1 Ry and the valley between the peaks becomes deeper by a factor of two. The present results are consistent with those calculated by the QMC+DMFT with use of the Hamiltonian without transverse spin fluctuations.²²

There is no XPS experimental data for the bulk γ -Mn. But, the photoemission data²² for the 20 monolayer fcc Mn on the Cu_3Au (100) are consistent with the results of calculations as shown in Fig. 3. The high-energy peak at $\omega = 0.1$ Ry may be justified by the BIS data,²³ although the data are taken for α -Mn at room temperature.

It should be noted that in the case of Ni the central peak of the t_{2g} bands in the LDA shifts to $\omega = -0.15$ Ry. Furthermore, the scattering magnitude $-\text{Im}\Sigma_{L\sigma}(\omega + i\delta)$ is weakened by a factor of ten or more as compared with the case of γ -Fe, and it is enhanced around $\omega = -0.45$ Ry instead of $\omega = -0.15$ Ry. Moreover the energy shift $\text{Re}\Sigma_{L\sigma}(\omega + i\delta) < 0$ for $\omega > -0.45$ Ry and $\text{Re}\Sigma_{L\sigma}(\omega + i\delta) > 0$ for $\omega < -0.45$ Ry. Therefore the valley found in the γ -Fe at $\omega = -0.1$ Ry disappears in the case of Ni. Instead, a small satellite peak appears around $\omega = -0.50$ Ry (6 eV satellite³).

We note that the Mott-Hubbard bands have recently been found in the Fe-based compound LaFeAsO. There Fe atoms form a two-dimensional square lattice. The DOS²⁴ calculated by the DMFT clearly show a two-peak structure with a deep depression around $\omega = -0.1$ Ry, which is essentially the same as the present results of calculations though the LaFeAsO system seems to be considerably stronger than the γ -Fe in Coulomb interaction strength.

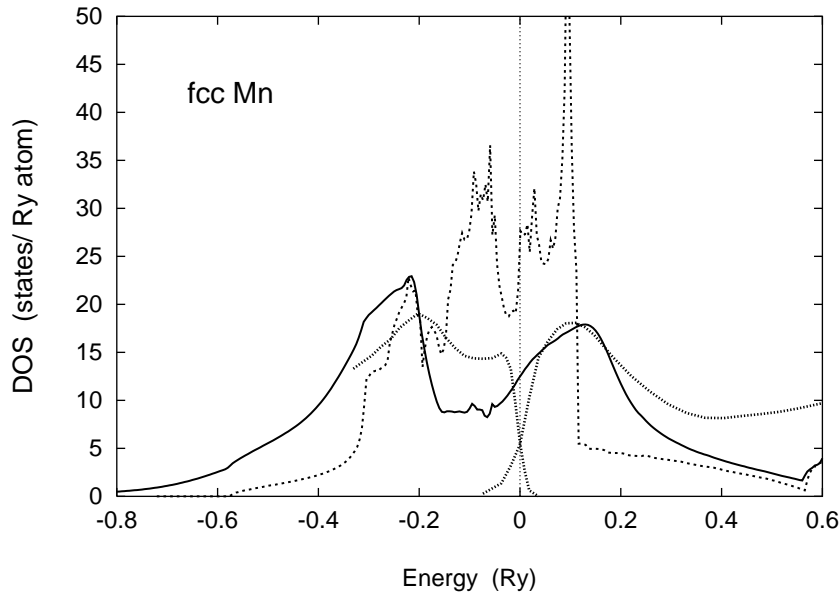


Fig. 3. The DOS for γ -Mn in the paramagnetic state (solid curve). The DOS in the LDA is shown by dashed curve. The XPS²² and BIS²³ data are shown by dotted curves.

In summary, we have calculated the DOS of single-particle excitation spectra for γ -Fe in the paramagnetic state on the basis of the first-principles dynamical CPA. We found that the γ -Fe shows the strong electron correlation effects on the single-particle excitations at high temperature region, *i.e.*, the disappearance of the central peak of the t_{2g} bands due to electron correlations and a formation of the Mott-Hubbard type bands. The result is quite different from the itinerant electron picture of γ -Fe obtained by the ground-state band calculations.⁵⁻⁷ Systematic investigations of the bulk fcc transition metals at high temperature region with use of the photoelectron spectroscopy are highly desired to verify the present results.

Acknowledgement

This work was supported by Grant-in-Aid for Scientific Research (19540408). Numerical calculations have been partly carried out with use of the Hitachi SR11000 in the Supercomputer Center, Institute of Solid State Physics, University of Tokyo.

References

- 1) See, for example, V.L. Moruzzi and C.B. Sommers: *Calculated Electronic Properties of Ordered Alloys: A Handbook* (World Scientific, Singapore, 1995).
- 2) Y. Kakehashi: *Adv. Phys.* **53** (2004) 497.
- 3) F.J. Himpsel, J.A. Knapp, and D.E. Eastman: *Phys. Rev. B* **19** (1979) 2919.
- 4) Y. Kamihara, T. Watanabe, H. Masahiro, and H. Hosono: *J. Am. Chem. Soc.* **130** (2008) 3296.
- 5) S. Fujii, S. Ishida and S. Asano: *J. Phys. Soc. Jpn.* **60** (1991) 4300.
- 6) K. Knöpfle, L. M. Sandratskii and J. Kübler: *Phys. Rev. B* **62** (2000) 5564.
- 7) E. Sjöstedt and L. Nordström: *Phys. Rev. B* **66** (2002) 014447.
- 8) Y. Kakehashi, T. Shimabukuro, T. Tamashiro, and T. Nakamura: *J. Phys. Soc. Jpn.* **77** (2008) 094706.
- 9) Y. Kakehashi: *Phys. Rev. B* **45** (1992) 7196; *Phys. Rev. B* **65** (2002) 184420.
- 10) O.K. Andersen, O. Jepsen, and G. Krier: in *Methods of Electronic Structure Calculations* ed. by V. Kumar, O.K. Andersen, and A. Mookerjee (World Scientific Pub., Singapore, 1994) p. 63.
- 11) M. Cyrot: *J. Phys. (Paris)* **33** (1972) 25.
- 12) J. Hubbard: *Phys. Rev. B* **19** (1979) 2626; *B* **20** (1979) 4584; *B* **23** (1981) 5974.
- 13) H. Hasegawa: *J. Phys. Soc. Jpn* **46** (1979) 1504; **49** (1980) 178.
- 14) Y. Kakehashi: *Phys. Rev. B* **66** (2002) 104428.
- 15) A. Georges, G. Kotliar, W. Krauth, M.J. Rosenberg: *Rev. Mod. Phys.* **68** (1996) 13.
- 16) A.I. Lichtenstein and M.I. Katsnelson, and G. Kotliar: *Phys. Rev. Lett.* **87** (2001) 067205.
- 17) F.J. Himpsel: *Phys. Rev. Lett.* **67** (1991) 2363.
- 18) M. Zharnikov, A. Dittschar, W. Kuch, C.M. Schneider, and J. Kirschner: *J. Magn. Magn. Mater.* **165** (1997) 250.
- 19) V.I. Anisimov, F. Aryasetiawan, and A.I. Lichtenstein: *J. Phys. Condens. Matter* **9** (1997) 767.
- 20) T. Bandyopadhyay and D.D. Sarma: *Phys. Rev. B* **39** (1989) 3517.
- 21) J.B. Mann: Los Alamos Scientific Laboratory Rep. No. LASL-3690 (1967).
- 22) S. Biermann, A. Dallmeyer, C. Carbone, W. Eberhardt, C. Pampuch, O. Rader, M.I. Katsnelson, and A.I. Lichtenstein: *condmat/0112430v1* (2001).
- 23) W. Speier, J.C. Fuggle, R. Zeller, B. Ackermann, K. Szot, F.U. Hillebrecht, and M. Campagna: *Phys. Rev. B* **30** (1984) 6921.
- 24) K. Haule, J.H. Shim, and G. Kotliar: *Phys. Rev. Lett.* **100** (2008) 226402.